

Model Climatology of the North American Monsoon Onset Period during 1980–2001

J. XU

Department of Hydrology and Water Resources, The University of Arizona, Tucson, Arizona

X. GAO

Department of Civil and Environmental Engineering, University of California, Irvine, Irvine, California

J. SHUTTLEWORTH

Department of Hydrology and Water Resources, The University of Arizona, Tucson, Arizona

S. SOROOSHIAN

Department of Civil and Environmental Engineering, University of California, Irvine, Irvine, California

E. SMALL

Department of Geological Sciences, University of Colorado, Boulder, Colorado

(Manuscript received 15 July 2003, in final form 20 February 2004)

ABSTRACT

In this study, the seasonal development of the North American monsoon system (NAMS), as simulated by a mesoscale model during a 22-yr simulation from 1980 through 2001, is assessed. Comparison between model simulations and observations shows that the model simulation reproduces the precipitation, skin temperature, and wind field patterns in the seasonal development (May–July) of the NAMS reasonably well and that the mesoscale features and spatial heterogeneity of the NAMS are described correctly. The onset of the monsoon in the central and southern Sierra Madre Occidental (SMO) in Mexico occurs on 20 June, about 2 weeks earlier than the onset in Sonora, Mexico (6 July), the Sonoran Desert, and central Arizona and New Mexico (8 July). The temperature in Mexico is highest after the onset of the monsoon and then decreases with the increasing monsoon rainfall. However, the temperature in the Sonoran Desert and central Arizona and New Mexico is highest just prior to the onset of the monsoon, and high temperatures may then persist throughout July. The lower-level (700 hPa) zonal wind field reverses from westerly to easterly over the central and southern SMO just before the onset of rain in these regions; this is associated with the abrupt northward movement of the subtropical high over this region. The progression of the subtropical high into central Arizona and New Mexico results in a local reduction in the westerly flow, and although the southwesterly flow weakens, atmospheric moisture is still mainly from the Gulf of California and the eastern Pacific Ocean.

1. Introduction

The North American monsoon system (NAMS) is currently receiving considerable attention in the hydro-meteorology community. This is partially because most of the monsoon region is arid or semiarid, such as Arizona and New Mexico, and is experiencing above-average rates of population growth. Supporting this development and, in particular, providing information of sustainable water resources for it is a critical issue. Pre-

dicting warm season precipitation in this region poses a considerable scientific challenge because the precipitation may be influenced by global climate variability and local surface heterogeneity.

As Fig. 1 shows, the NAMS region is characterized by two large upland areas: the Colorado Plateau, which extends northward and eastward from the Mogollon Rim in Arizona to the Rocky Mountains, and the Mexican Plateau, which is defined to the west and east by the Sierra Madre Occidental (SMO) and Oriental, respectively. The entire region has been called the North American Plateau (Tang and Reiter 1984). In addition, the peninsular ranges of southern California and Baja California play an important role in the climatology of the interior deserts by limiting penetration of marine

Corresponding author address: Dr. Xiaogang Gao, Department of Civil and Environmental Engineering, University of California, Irvine, Irvine, CA 92717.
E-mail: Gaox@uci.edu

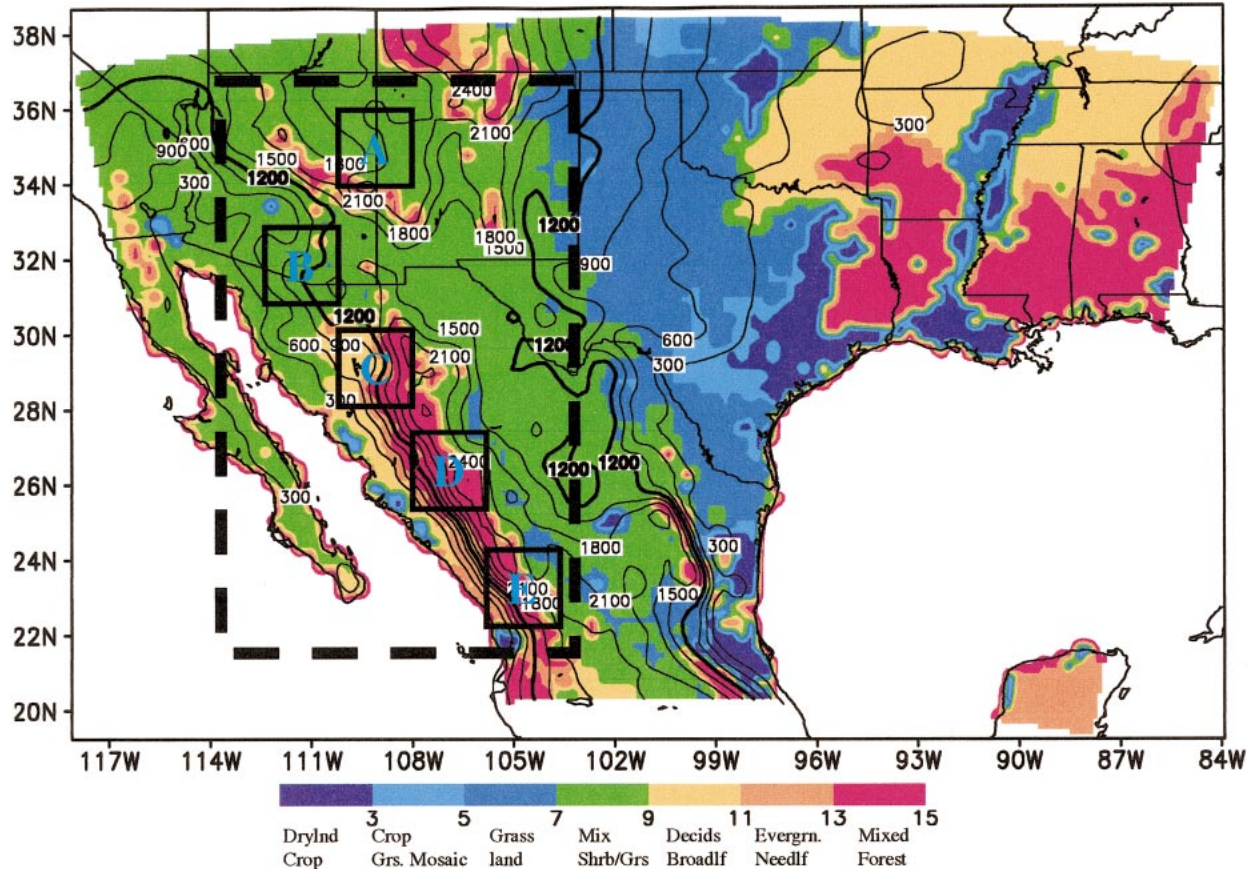


FIG. 1. The fine-domain regions used in the MM5 simulations. The box marked with a thick dashed line shows the core of the North American monsoon region as defined in this analysis. Contours are used to indicate elevation, and color is used to describe the type of vegetation represented in the model. Five subareas are defined and referred to in the text as follows: (A) the northern Mogollon Rim on the interface between Arizona and New Mexico (34° – 36° N, 108° – 110° W), (B) portions of the Sonoran Desert (31° – 33° N, 110° – 112° W), (C) portions of Sonora north of the SMO (28° – 30° N, 108° – 110° W), (D) portions of Sinaloa near the middle of the SMO (25° – 27° N, 106° – 108° W), and (E) portions of Nayarit south of the SMO (22° – 24° N, 104° – 106° W).

moisture from the Pacific Ocean. There are also two lowland areas associated with the NAMS: the lower Colorado River valley and neighboring low desert areas, which play a critical role in the formation of the thermal low, and the coastal lowlands of Sonora and SinaloaMexico, between the Gulf of California and the western flanks of the SMO. Consistent with the complex terrain, vegetation exhibits a substantial spatial difference. A narrow strip along the western slope of the SMO is covered by mixed forest, while, in stark contrast, central Mexico and most of the southwestern United States are covered with grass or shrubland. The large spatial variability in precipitation that results from the complicated geography and vegetation has made it difficult to document and understand the major elements of the NAMS and their evolution at seasonal and interannual time scales.

Global atmospheric reanalysis data, gauge, and satellite data have been analyzed to provide some understanding of the life cycle, large-scale features, and

mechanisms involved in the NAMS (Tang and Reiter 1984; Carleton 1986; Douglas et al. 1993; Schmitz and Mullen 1996; Adams and Comrie 1997; Higgins et al. 1997; Barlow et al. 1998). However, spatially heterogeneous features of precipitation and regional-scale circulation remain poorly described due to the lack of adequate in situ and observational data and the limited horizontal resolution of the [National Centers for Environmental Prediction (NCEP) and European Centre for Medium-Range Weather Forecasts (ECMWF)] reanalysis data.

Because of these regional-scale features, studies using regional models are becoming important, but previous modeling studies for the NAMS are far from perfect. Earlier simulations (e.g., Giorgi 1991; Giorgi et al. 1994) of the Sonoran region missed many important features of the monsoon, such as the maximum summer precipitation being over western Mexico (Schmitz and Mullen 1996). Dunn and Horel (1994a, b) discovered problems in the Eta Model's boundary layer scheme that

caused model forecasts of convection in Arizona to verify poorly. Although Stensrud et al. (1995) used the fifth-generation Pennsylvania State University–National Center for Atmospheric Research (PSU–NCAR) Mesoscale Model (MM5; without a land surface scheme) and successfully reproduced many NAMS characteristics, including the large-scale midtropospheric wind fields, southerly low-level winds over the Gulf of California, and the heavy rains over western Mexico, their integrations were limited to less than 24 h. As mesoscale models have developed, more recent studies have provided encouraging results. A series of simulations of the dynamics of low-level circulation over the southwestern United States and northwestern Mexico were conducted by Anderson (2002) and Anderson et al. (2000a,b, 2001) using a regional spectral model (RSM). By coupling an RSM with a land surface model, Kanamitsu and Mo (2003) pointed out that the large-scale distribution of soil wetness over the western United States plays a significant role in determining the precipitation variability of the southwestern monsoon. Using Eta Model mesoscale analyses and forecasts for three summer seasons (July–September 1995–97), Berbery (2001) analyzed the precipitation patterns estimated from satellite data and pointed out that the diurnal cycle must be captured if the interaction between monsoon circulation and precipitation is to be resolved. Using the MM5 model, Gochis et al. (2002, 2003) investigated the role of convective parameterization schemes in the simulation of NAMS. Meanwhile, Xu and Small (2002) emphasized the relevance of the combination of convective parameterization schemes and radiation schemes and pointed out that the Grell et al. (1994) convective parameterization and rapid radiative transfer model (RRTM) seem to produce the most realistic patterns and magnitudes of rainfall in the NAMS region in their modeling studies. A report (Gutzler et al. 2004) documents a set of model output results generated by six independent modeling groups and shows the seasonal evolution and diurnal cycle of precipitation, surface flux, and temperature, and low-level wind fields for the 1990 summer season. However, many previous studies focus only on a specific year, and NAMS climatologies calculated from long-term regional model simulations are rare in the literature.

In this study, the ability of the MM5 model coupled Oregon State University (OSU) land surface model to simulate the seasonal development of the NAMS at a regional scale is examined during a 22-yr simulation from 1980 through 2001. The model output is compared with the NCEP/NCAR reanalysis data, gauge precipitation products from the U.S. Climate Prediction Center (CPC), and the Television Infrared Observation Satellite (TIROS) Operational Vertical Sounder (TOVS) skin temperature data for 22 yr.

The model and observation datasets used in this study are introduced in sections 2 and 3, respectively. The validation of the simulated climatology is described in

section 4. The onset of the monsoon and the evolution of precipitation, skin temperature, and wind fields are investigated in section 5, and the circulation associated with the seasonal development of NAMS is explored in section 6. Conclusions and a discussion are summarized in section 7.

2. Model and simulations

The MM5 coupled to the OSU land surface model (Chen and Dudhia 2001) used in this study is a limited area, nonhydrostatic mesoscale atmospheric model (Grell et al. 1994) with terrain-following vertical coordinates (σ). Several parameterizations are available for the convective precipitation and radiation schemes and the atmospheric boundary layer. The OSU Land Surface Model (LSM) is capable of predicting soil moisture and temperature in four layers (10, 30, 60, and 100 cm thick) as well as canopy moisture and water-equivalent snow depth. The model also computes the accumulation of surface and underground runoff. The LSM recognizes vegetation and soil type when calculating evapotranspiration and includes the effect of soil conductivity and the gravitational flux of moisture. In MM5, the LSM can be used instead of the SLAB model and provides the surface fluxes to the planetary boundary layer (PBL) scheme using surface layer exchange coefficients along with radiative forcing and the precipitation rate as input parameters. The LSM uses a diagnostic equation to obtain skin temperature and the exchange coefficients for heat and moisture transfers (Chen et al. 1997; Chen and Dudhia 2001).

a. Domain selection, period of simulation, and boundary conditions

A 90-km coarse grid was used to allow realistic representation of low-level flow from both the Pacific Ocean/Gulf of California and the Gulf of Mexico regions. A 30-km, two-way nested grid centered over the NAMS region (Fig. 1) was then used to give better representation of the regions' complex topography and associated spatial variability in surface characteristics. It is the model output from this fine domain that is analyzed and validated in the model present study. To assess seasonal and interannual variability, simulations were made for the period 1 May through 31 July each year between 1980 and 2001 using the same model setup. The initial conditions were specific on 1 May in each year.

The initial atmospheric and surface fields and boundary conditions, including soil moisture and temperature for the coarse domain, were taken from the NCEP–NCAR reanalysis dataset (Kalnay et al. 1996). The lateral boundary conditions are time dependent. The outer two rows and columns in the parent domain have specified values of all predicted fields from the reanalysis datasets, and the counterpart in the nest domain is sup-

plied by the parent domain. Our previous studies and the results of Kanamitsu and Mo (2003) suggest that model precipitation, soil moisture, and skin temperature have limited sensitivity to such initial conditions. The PBL was modeled using the high-resolution Blackadar scheme. Land use at each grid point was defined among 24 categories (ranging from urban land to snow or ice), with climatological values of associated physical properties (albedo, moisture availability, emissivity, roughness length, and thermal inertia) assigned according to the category and time of year (Grell et al. 1994). Vertical levels were arranged so that the model output is available at 23 levels (0.995, 0.985, 0.970, 0.945, 0.910, 0.870, 0.825, 0.775, 0.725, 0.675, 0.625, 0.575, 0.525, 0.475, 0.425, 0.375, 0.325, 0.275, 0.225, 0.175, 0.125, 0.075, and 0.025) to the top of the atmosphere, with a relatively higher concentration at the lowest levels to better resolve the planetary boundary layer structure.

b. Convection and radiation parameterizations

There is a wide variety of physical parameterization schemes available in the MM5 modeling system, and modeling results with each physical parameterization scheme are likely sensitive to the domain size, grid resolution, and location studied. In previous work (Xu and Small 2002), we compared results from a combination of two convection schemes [Grell and Kain–Fritsch (1990)] and three radiation schemes [Community Climate Model, version 2 (CCM2), cloud-radiation scheme, and RRTM]. Differences in simulated rainfall produced by the various combinations of schemes are substantial. The Grell–RRTM simulation produces the most realistic patterns and magnitudes of rainfall, including intraseasonal variations and the differences between the wet and dry years. Simulations using the Kain–Fritsch scheme produce too much rainfall and fail to represent the typical observed decrease in precipitation from June to July. The CCM2 radiation scheme produces a simulated climate that is too cloudy, yielding little rainfall in the NAMS region regardless of the convection scheme used. Consequently, the Grell cumulus convective parameterization (Grell 1993) and RRTM radiation schemes were considered most appropriate when describing the NAMS.

3. Observed and analyzed datasets

- *Precipitation.* The observed precipitation data are taken from the CPC real-time analysis dataset (Higgins et al. 1996), which is derived from the 6000 gauges in the U.S. Cooperative Observing Network interpolated onto $1^\circ \times 1^\circ$ grids. The data were available for the whole model domain in the United States and Mexico.
- *Skin temperature.* The skin temperature data are taken from the TOVS Pathfinder $1^\circ \times 1^\circ$ gridded dataset,

which is available at least twice a day depending on the number of satellites available. Skin temperature is derived using the infrared and thermal channels (8, 18, and 19) of the High-Resolution Infrared Sensor (HIRS) instrument. This dataset (Susskind and Lakshmi 1997) has been validated (Lakshmi et al. 1998; Lakshmi and Susskind 2000) in some regions by comparison with the skin temperature collected from field experiments.

- *Wind field.* Wind fields are taken from the NCEP–NCAR reanalysis product (Kalnay et al. 1996), which is gridded to a horizontal resolution of $2.5^\circ \times 2.5^\circ$.

4. Validation of simulated climatology

The simulated and observed average monthly precipitation, skin temperature, and wind fields were compared for May, June, and July from 1980 through 2001.

a. Precipitation

In May, the observed precipitation (Fig. 2a) is the greatest outside the NAMS region in the southern Great Plains (SGP), including Alabama, Mississippi, Louisiana, and Texas, along with substantial precipitation in eastern Mexico. Precipitation is relatively low across the whole NAMS areas. In June (Fig. 2b), the precipitation pattern is similar to that in May, but there is also substantial precipitation in southern Mexico and some over the SMO as the monsoon builds from southern Mexico. By July (Fig. 2c), the 1 mm day^{-1} isohyet has extended northward to include all of New Mexico and a portion of southeastern Arizona. The monthly precipitation exceeds 100 mm over the western slope of the SMO and exceeds 60 mm over the Sonoran Desert, but precipitation decreases noticeably toward the east of the study area. This result indicates that the monsoon occurs completely over the entire NAMS region.

Comparison of Figs. 2a–c with Figs. 2d–f shows that the model simulations capture the climatological patterns of precipitation well for 1980 through 2001. The abrupt increases in precipitation over the SMO in Mexico in June and the subsequent extension into the southwestern United States in July are well reproduced. In particular, mesoscale features of precipitation over the western slope of the SMO in June and July are described (Figs. 2e,f). As modeled precipitation increases in the NAMS region, it significantly decreases in the eastern portion of the study area, a feature that is similar to that observed in the study of Higgins et al. (1997).

To investigate the spatial heterogeneity of precipitation in the NAMS region, five representative subareas are compared (Fig. 1); they are defined as north of the Mogollon Rim on the interface between Arizona and New Mexico (A; $34^\circ\text{--}36^\circ\text{N}$, $108^\circ\text{--}110^\circ\text{W}$); the Sonoran Desert (B; $31^\circ\text{--}33^\circ\text{N}$, $110^\circ\text{--}112^\circ\text{W}$); Sonora, north of the SMO (C; $28^\circ\text{--}30^\circ\text{N}$, $108^\circ\text{--}110^\circ\text{W}$); Sinaloa, middle

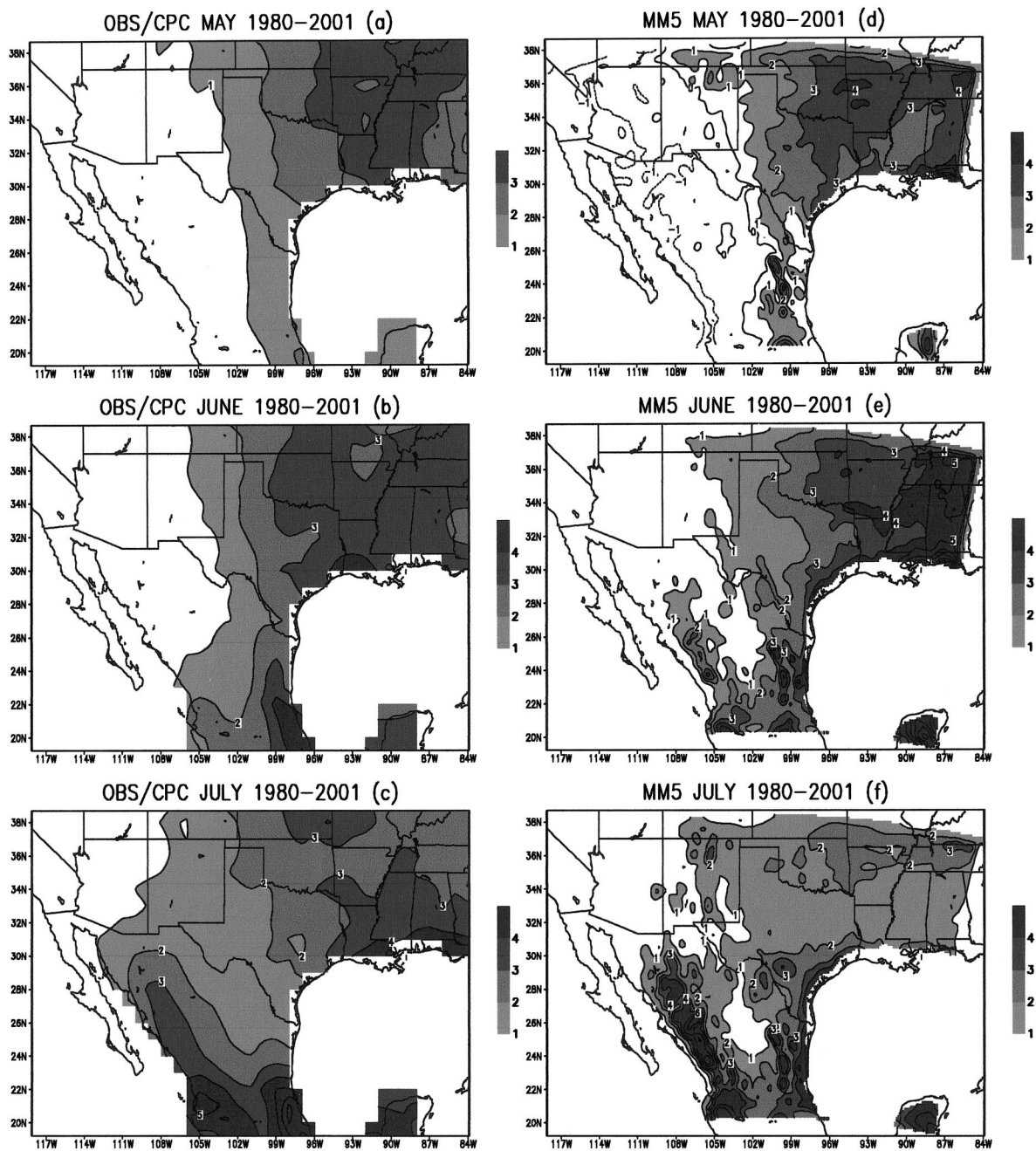


FIG. 2. The monthly average precipitation for the period of 1980–2001 in mm day^{-1} from observations (NCEP CPC) for (a) May, (b) Jun, and (c) Jul and calculated by MM5 for (d) May, (e) Jun, and (f) Jul.

of the SMO (D; 25° – 27°N , 106° – 108°W); and Nayarit, Mexico, south of the SMO (E; 22° – 24°N , 104° – 106°W).

Figure 3 shows the monthly average precipitation over these five regions. For the two northern NAMS regions (marked A and B in Fig. 1), the simulated precipitation in June and July is slightly lower than observed. For the three southern NAMS regions (marked C, D, and E in Fig. 1), the simulated precipitation is close to observations but is overestimated in the central

SMO. The fact that precipitation in the southern NAMS is much higher than in the northern NAMS is evident in both observations and model simulations.

In summary, in most areas, the model simulations correctly reproduce the seasonal development of the precipitation patterns during the NAMS, but the precipitation amounts are under- and overestimated in some areas. In particular, the seasonal development (from June to July) of precipitation in the NAMS region is captured

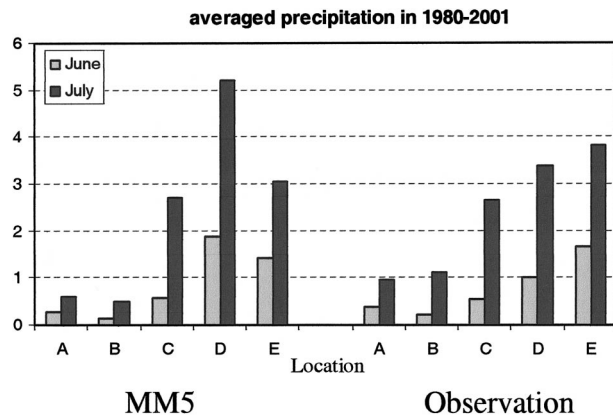


FIG. 3. Climatological monthly average precipitation in mm day^{-1} for the period of 1980–2001 for Jun and Jul from observations and MM5 simulations for the five subareas A, B, C, D, and E shown in Fig. 1.

roughly, and the mesoscale features and spatial heterogeneity of rainfall are described.

b. Skin temperature

In May, the TOVS skin temperature field (Fig. 4a) shows a large area of higher temperature (above 297 K), which spans northern Mexico and southwestern Arizona. A warm center (marked W) above 300 K extends from the Sonoran Desert to areas of Sonora. Temperature is lower (less than 294 K) throughout northern Arizona and New Mexico and most of the SGP. A strong cold center (marked C) is observed in the southern Colorado Plateau, with a narrow cold band (the dashed curve) in central Mexico between the Sierra Madre Oriental and the Sierra Madre Occidental. In June (Fig. 4b), the temperature pattern is similar to that in May. However, the temperature rises to a maximum of 306 K in the Sonoran Desert and other central areas of the NAMS region, while the temperature in the cold band decreases to 291 K. In July (Fig. 4c), the temperature in the northern region of the NAMS, including the southwestern United States and northwestern Mexico, continues to rise, while, interestingly, the temperature of the cold band in the southern NAMS region continues to fall.

When compared to the TOVS temperature field (Figs. 4a–c), the simulated results (Figs. 4d–f) show that the model captures the overall temperature patterns for the climatology for the years 1980–2001 fairly well. An area in the northern portion of the Gulf of California is an exception; here, the simulated temperature is slightly higher than the TOVS observations.

An interesting feature is present in both the observations and model simulations. As the precipitation shifts northward during the seasonal development of the monsoon, the temperature falls in the southern NAMS areas, and a cold center forms over the Mexican Plateau. In contrast, the temperature increases in the northern NAMS regions, with a warm center in the Sonoran De-

sert. Spatial heterogeneity is also found in the modeled skin temperature fields.

c. Atmospheric circulation

The 700-hPa wind field was chosen to compare the evolution of the NAMS in simulations and observations because it is the lowest above-surface level available throughout the NAMS region. A separate study (Xu and Small 2002) suggested it was representative to analyze the low-level troposphere moisture flow.

In May, the whole NAMS region is dominated by southwesterly flow in the NCEP–NCAR reanalysis field (Fig. 5a), with some anticyclonic flow in southern Mexico areas. This circulation suggests that, on average, the eastern Pacific Ocean and the Gulf of California are the primary moisture sources for the entire NAMS region. In June (Fig. 5b), a high pressure ridge (indicated by zero speed for the zonal wind in Fig. 5) appears from the northern Gulf of Mexico, through southern Texas and northern Mexico, to the eastern Pacific Ocean, with easterlies dominating in southern areas. Northern Mexico and the southwestern United States are still under the control of southwesterlies. These, albeit average, flow fields suggest that moisture from the Gulf of Mexico contributes little in the northern NAMS region, with most moisture from the Gulf of Mexico being transported into southern Mexico and the southeastern United States. By July (Fig. 5c), the high pressure ridge shifts northward, and moisture from the Gulf of Mexico can reach all of Mexico. Moisture is transported into the southwestern United States from the Gulf of California and the eastern Pacific Ocean, but slightly less than in June.

In May, model simulation (Figs. 5d–f) is generally representative of the NCEP–NCAR reanalysis wind field (Figs. 5a–c), and southwesterly flow is simulated over the entire study area (Fig. 5d). In June (Fig. 5e) and July (Fig. 5f), the anticyclonic flows over the northern Gulf of Mexico, southern Texas, and northern Mexico are also identified in the simulation, but there is a substantial and interesting difference between the simulations and the reanalysis field. In the simulations, the circulation has more finescale structure than is presented in the NCEP–NCAR reanalysis fields, and the complexity of the within-the-zero-speed area over the Mexican Plateau is revealed because of the higher resolution of the MM5–OSU model.

5. Onset of North American monsoon

- *Precipitation.* The average simulated precipitation index (PI) over the five subareas (Fig. 3) is used to explore the heterogeneity of the precipitation in the NAMS region. The PI time series for these five regions are shown in Fig. 6. The date of onset was determined in the same way as Higgins et al. (1997); however,

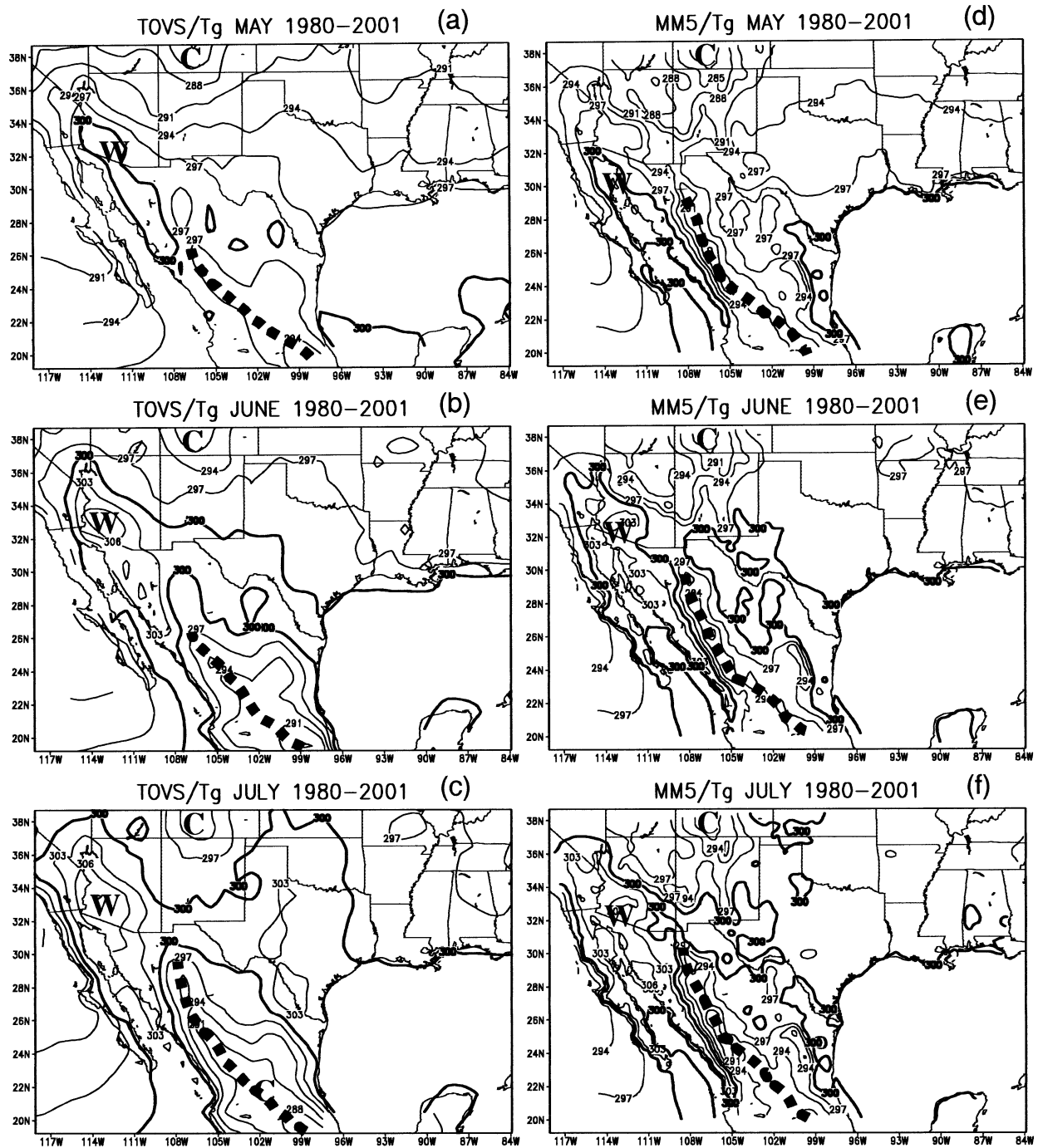


FIG. 4. Monthly average skin temperatures for the period of 1980–2001 in kelvins from observations (TOVS) for (a) May, (b) Jun, and (c) Jul and calculated by MM5 simulations for (d) May, (e) Jun, and (f) Jul. Here, “C” indicates the cold center, and “W” indicates the warm center. Dashed lines indicate the band of cold.

because precipitation in Mexico is much higher than in the southwestern United States (Fig. 3), the criteria for onset use different values in different areas. For the two northern NAMS regions (A and B), the magnitude of precipitation and duration criteria used to determine onset were $+0.5 \text{ mm day}^{-1}$ and 3 days,

respectively; for the three southern NAMS regions (C, D, and E), the precipitation and duration criteria used were $+2.0 \text{ mm day}^{-1}$ and 3 days, respectively.

In the northern NAMS region, the simulated precipitation increases considerably in early July (Fig. 6a) and, using the above criteria, the date of monsoon

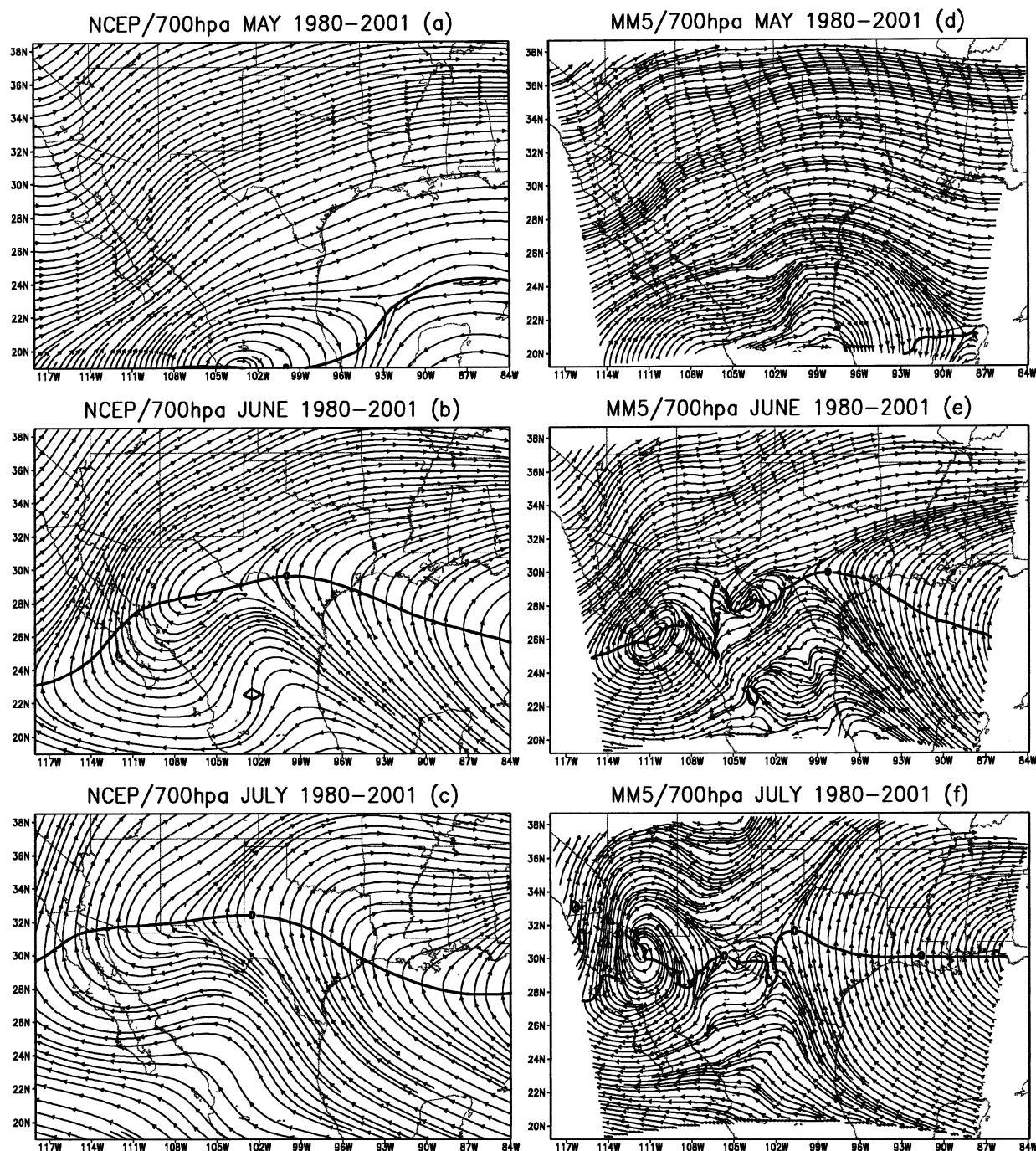


FIG. 5. Average monthly wind (m s^{-1}) fields at 700 hPa for the period 1980–2001 from NCEP–NCAR reanalysis for (a), May, (b) Jun, and (c) Jul and from MM5 simulations for (d), May, (e) Jun, and (f) Jul. The thick solid line represents the zero speed of zonal wind and marks the location of the ridge of anticyclonic flow.

onset in both the Sonoran Desert and central areas of Arizona and New Mexico is 8 July, which is similar to observations [7 July was defined in the study of Higgins et al. (1997)]. Following this initial rise in A and B the simulated precipitation index oscillates irregularly. In contrast, the precipitation index increases

dramatically at the end of June in Mexican areas (Fig. 6b). The onset of the monsoon in central Mexico (D) and the southern SMO (E) occurs, on average, on 20 June, while the date of monsoon onset in the Sonora Desert (C) is 6 July, almost the same time as in the northern NAMS region. Thus, the onset of the mon-

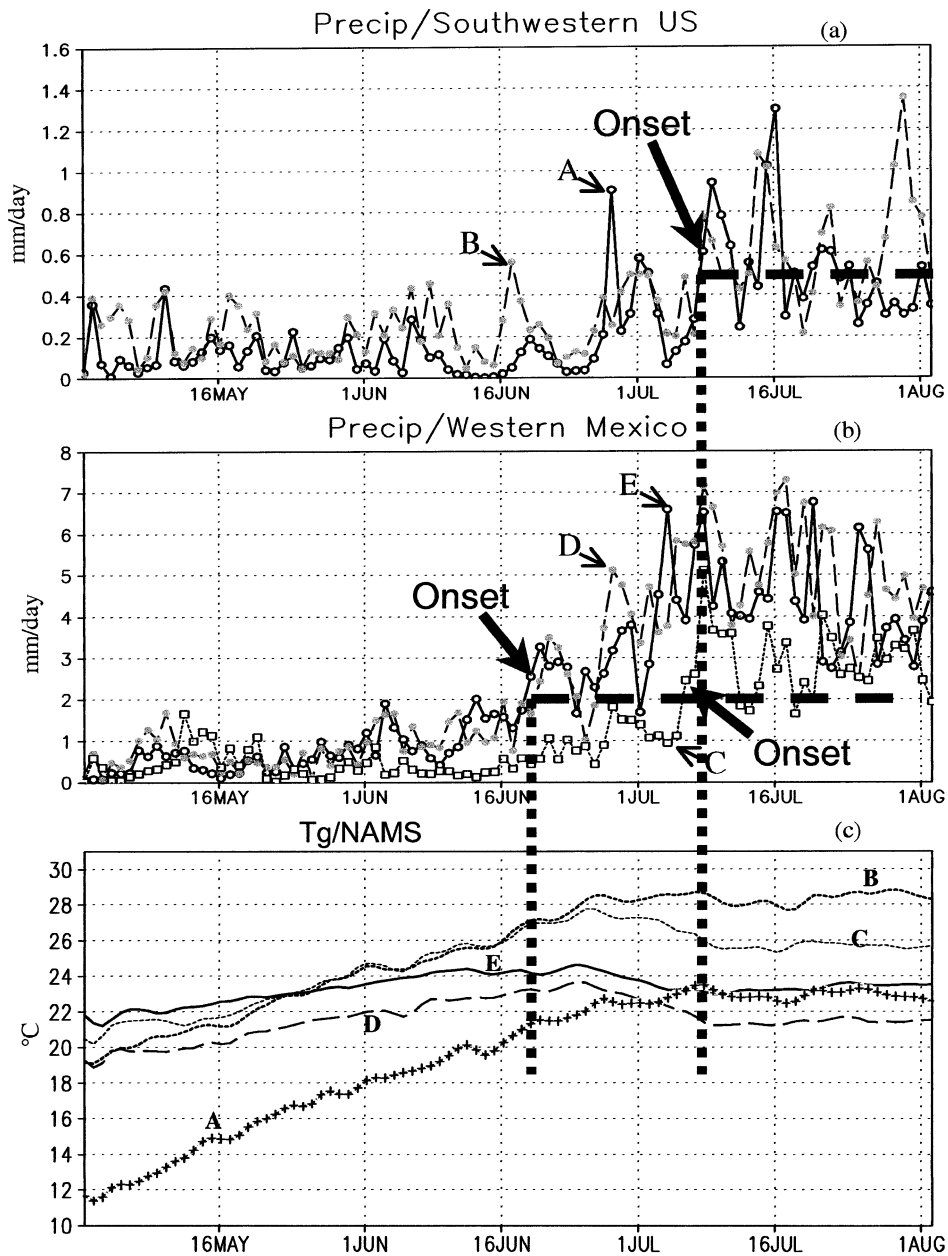


FIG. 6. Time series of simulated daily precipitation (mm day^{-1}) and skin temperatures ($^{\circ}\text{C}$) in the five subareas over the NAMS region defined in Fig. 1 for the period 1 May–31 Jul. (a) Precipitation in the southwestern United States (A and B), (b) precipitation in western Mexico (C, D, and E), and (c) surface temperature in all five subareas (A, B, C, D, and E).

soon in central Mexico and south of the SMO is, on average, 2 weeks earlier than in the southwestern United States and northwestern Mexico.

- *Skin temperature.* In Mexico (D and E in Fig. 6c), the temperature rises 4–5 days after the monsoon onset in Mexico and then decreases by 2°C with increasing monsoon rainfall. This result is consistent with observations in the study by Douglas et al. (1993). However, the temperatures in the Sonoran Desert (B in Fig. 6c) and in central Arizona and New Mexico (A in Fig.

6c) are highest just prior to the onset of the monsoon, and high temperatures persist throughout July. It is worth noting that the temperature north of the SMO (C) follows a similar evolution as the other Mexican areas (D and E); however, the evolution in precipitation is more similar to regions A and B. In this way, seasonal temperature variations in the southwestern United States are quite different from those in Mexico.

- *Wind field.* Consistent with the seasonal development of NAMS described above, the low-level zonal wind

field (at 700 hPa) reverses direction from westerly to easterly in the central and southern SMO areas before the onset of rain (D and E in Fig. 7a). Meanwhile, the (westerly) wind speed decreases to almost zero in the northern SMO (C) and reduces significantly in the southwestern United States (A and B). It is interesting that meridional low-level flow (Fig. 7b) is southerly in all five areas and does not increase with the northward development of precipitation along the western slope of the SMO, through the Sonoran Desert, to central Arizona and New Mexico. Westerly (Fig. 7c) and southerly (Fig. 7d) wind speeds at upper levels (200 hPa) mimic those at lower levels and decrease substantially in all areas with the development of NAMS, but the reversal zonal wind does not occur.

- *Precipitable water.* In response to the change in atmospheric circulation, the moisture content of the air increases consistently with the onset of the monsoon across the entire NAMS area (Fig. 8). This increase persists throughout the monsoon everywhere, but the moisture content in southern Mexico is roughly twice that in central Arizona and New Mexico.

6. Subtropical high movement associated with the development of NAMS

The comparison of simulated and observed precipitation, skin temperature, and circulation described above shows that model simulations reproduce the climatological spatial distributions and seasonal development of the NAMS very well. Previous research, based mainly on coarse resolution and large-scale NCEP and ECMWF reanalysis data, discuss the evolution of the NAMS, but an analysis of the simulated fields calculated by a mesoscale model may provide a better understanding of more complex aspects of the NAMS.

Pioneering research by Bryson and Lowry (1955) pointed out that the onset of summer rains in Arizona is associated with the change from westerlies to easterlies in the midtroposphere. Their explanation is that air from the east or southeast, traveling around a westward extension of the Bermuda high, carries greater moisture content (originating over the Gulf of Mexico) than air from the west or southwest. Although this explanation was disputed by subsequent studies (Reitan 1957; Hales 1972; Carleton 1986), there is substantial evidence that monsoon onset is closely related to the subtropical high in the NAMS region. In the simulated climatology of the mesoscale model, circulation associated with the subtropical high at the midlevels (500 hPa) and the low levels (700 hPa) was examined.

a. Potential height time–latitude cross NAMS section

To understand the activity of the subtropical high during the seasonal development of NAMS more clearly, the time evolution of potential height over the NAMS

sections (104°–112°W) was analyzed. There is evidence (Fig. 9) of a high center (with a maximum value of 5880 gpm) over the south of the SMO (~21°N) in early June. About 5–10 days before the onset of the monsoon in southern Mexico, the contour of 5880 gpm moves northward to Sonora (~28°N) and then enlarges northward, while the high at the south of the SMO enhances to 5900 gpm when the monsoon develops. The movement of the subtropical high corresponds to the wind reversal from westerly to easterly over the central and southern SMO (see D and E in Fig. 7). The center of the subtropical high persists in Sonora for 2 weeks, then moves rapidly northward to central Arizona and New Mexico (~34°N) a few days earlier than the local onset of the monsoon, and westerlies reduce over the Sonoran Desert and southwestern United States (see A, B, and C in Fig. 7).

b. Evolution of circulation with the onset of monsoon

The 5-day mean potential height at 500 hPa and wind fields and water vapor mixing ratio at 700 hPa were analyzed to investigate the relationship between the movement of the subtropical high and the onset of NAMS. As mentioned before, 700 hPa is the lowest level above the surface throughout the NAMS region. Before the onset of the NAMS (11–15 June), the entire SMO area is dominated by the 500-hPa subtropical high, with a maximum value of around 5880 gpm, while a weak trough lies over the western coast of the Gulf of Mexico (Fig. 10a). At the same time, lower-tropospheric circulation (Fig. 10b) is dominated by an anticyclone, which is centered over the southern Gulf of California and western slopes of the SMO. A region of zero wind extends east–west over central Mexico and the northern Gulf of Mexico, with easterlies and westerlies on either side, the northern westerlies being much stronger than the southern easterlies. The peak water vapor mixing rate is centered at the same latitude (20°–22°N) as the easterlies, associated with the moisture from the Gulf of Mexico.

At the time of the onset of the monsoon in southern Mexico (21–25 June), a subtropical high of 5890 gpm appears over Sonora and increases substantially in intensity (Fig. 10c). The meridional extent of the subtropical high over the NAMS region is associated with the deepening of the trough over the south-central United States. Meanwhile, the 700-hPa anticyclonic ridge moves northward to north of the SMO and central Texas (Fig. 10d). There is a northward advance of the easterlies, and the water vapor content of air increases remarkably over central and southern Mexico, consistent with the local onset of the monsoon. This result indicates that the onset of the monsoon over southern Mexico is significantly affected by the northward movement of the subtropical high, the expansion of the tropical easterlies, and an associated increase in water vapor content.

By the time of onset of the monsoon in the southwestern United States (6–10 July), the 5880-gpm iso-

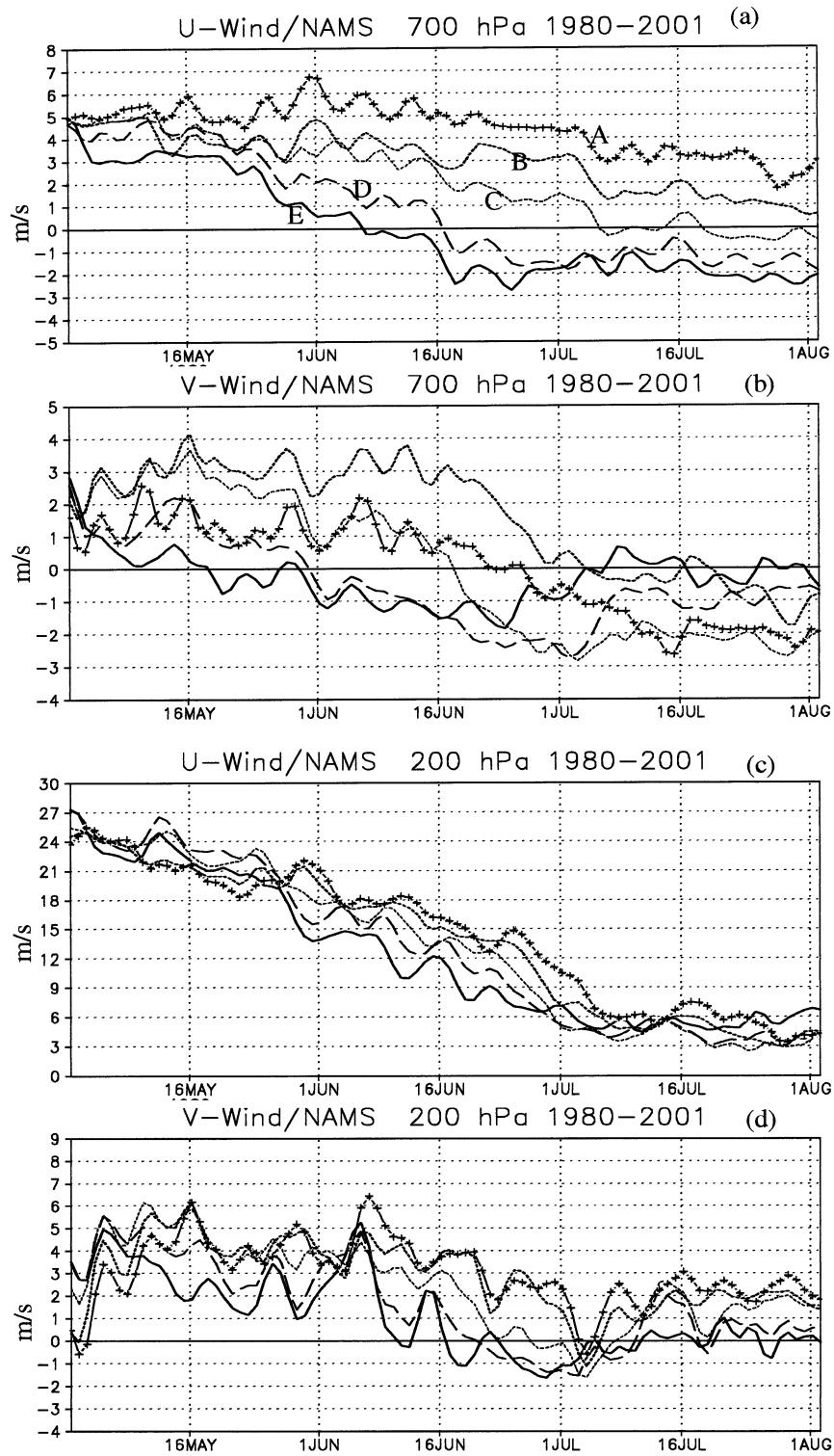


FIG. 7. Same as in Fig. 6, except for (a) zonal wind (m s^{-1}), (b) meridional wind (m s^{-1}) at 700, (c) zonal wind at 200, and (d) meridional wind at 200 hPa.

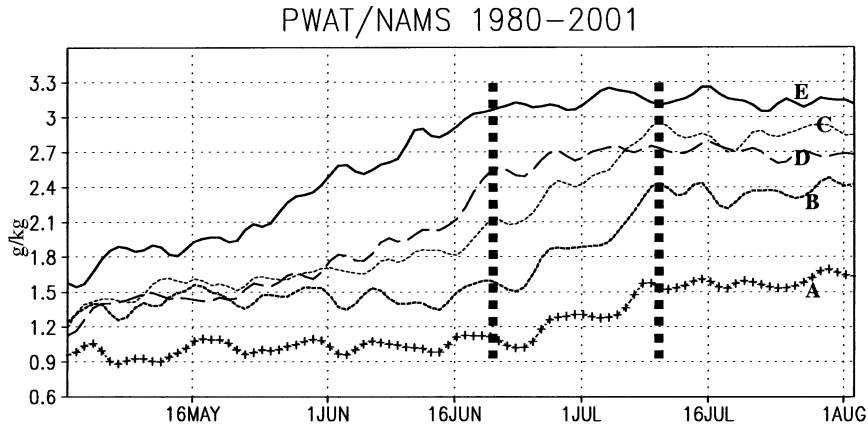


FIG. 8. Same as in Fig. 6, except for precipitable water vapor (g kg^{-1}).

hypse in the 500-hPa potential height field dominates the entire study area, centered over the central southwestern United States (Fig. 10e). As the 700-hPa ridge continues northward, easterlies prevail over most of Mexico (Fig. 10f), the southwesterlies reduce in northern Arizona and New Mexico, water vapor content increases continuously reaching 5 g kg^{-1} over most of the North American plateau (i.e., above 1200 m in Fig. 1), and the southerlies associated with the Great Plains jet stream strengthen in the lee of the Rockies.

The elevated subtropical anticyclone over the North American plateau clearly profoundly impacts the development of the monsoon in Mexico and the southwestern United States by modulating the configuration of atmospheric circulation. The 700-hPa easterlies over southern Mexico are responsible for much of the westward moisture transport from the Gulf of Mexico into the central and southern SMO but appear to make a limited contribution in the southwestern United States, where moisture originates mainly from the low-level southwesterlies over the Gulf of California and the eastern Pacific Ocean.

7. Summary and discussion

a. Summary

In this study, the MM5 model linked to the OSU land surface scheme was used to assess the seasonal variation of the North American monsoon averaged in a 22-yr simulation from 1980 through 2001. Model simulations were compared to the rain gauge precipitation data derived by National Centers for Environmental Prediction (NCEP), and TOVS skin temperature data were derived by High-Resolution Infrared Sensor and NCEP-NCAR four-dimensional assimilation reanalysis wind field data. The results show that the MM5-OSU model simulation reproduces the seasonal development (May-July) of the precipitation, skin temperature, and wind field patterns very well and provides a plausible description of mesoscale-scale features and spatial heterogeneity within the NAMS.

Precipitation in the five subareas was investigated. The results show that, in the central and southern Sierra Madre Occidental areas, the onset of the monsoon occurs on 20 June, about 2 weeks earlier than the onset

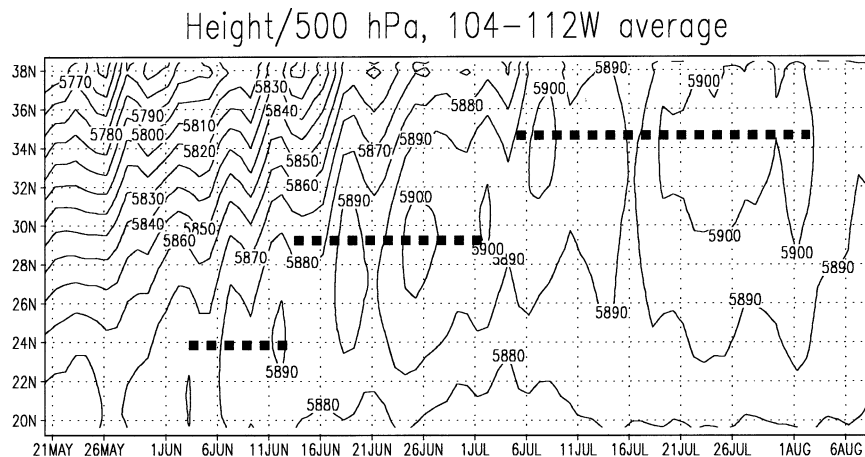


FIG. 9. The time-latitude section of potential height (gpm) at 500 hPa averaged over the region 104° - 112° W. The dashed lines indicate roughly the location of the high subtropical center.

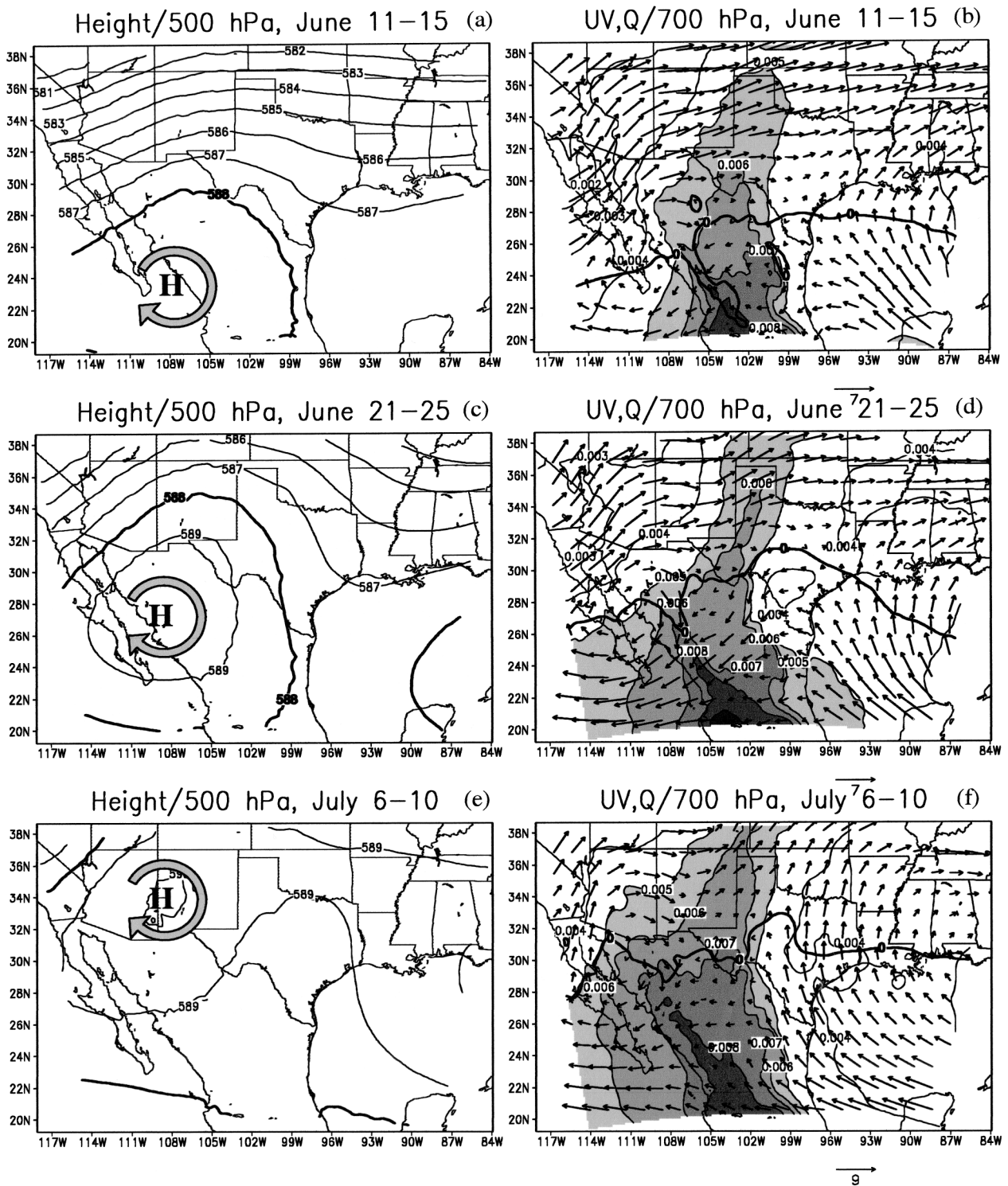


FIG. 10. The 5-day average of the MM5 simulated potential height (gpm) at 500 hPa for (a) 11–15 Jun, (c) 21–25 Jun, and (e) 6–10 Jul, and the vector of wind field and water vapor mixing rate (shaded; kg kg⁻¹) at 700 hPa for (b) 11–15 Jun, (d) 21–25 Jun, and (f) 6–10 Jul.

in Sonora (6 July), Sonoran Desert, and the central southwestern United States (8 July), a result which is close to observations (7 July).

With the seasonal development of NAMS, the temperature in Mexico is higher after the monsoon onset and then decreases with an increase in monsoon rainfall. However, the temperature in the Sonoran Desert and central areas of Arizona and New Mexico is highest immediately prior to the monsoon onset, and higher temperatures persist through July. Temperature in the southwestern United States did not decrease with an increase in monsoon rainfall, which is quite different from the behavior in Mexico.

Zonal wind fields at 700 hPa reverse from westerly to easterly in the central and southern SMO areas before the onset of rainfall. Meanwhile, the speed of westerlies decreases to almost zero in the northern SMO and reduces significantly in the southwestern United States, while westerlies in the upper level (200 hPa) decrease substantially over the entire NAMS; however, the reversal in zonal winds was not found. With the change in wind direction, the water content of the air consistently increases with the onset of the monsoon across the NAMS region and remains constant during the monsoon.

The onset of the NAMS is closely related to a rapid northward movement of the midlevel (500 hPa) subtropical high over the North American plateau, which occurs 3–10 days before the local monsoon onset. The initial movement of the subtropical high from south to north of the SMO is consistent with wind reversal from westerly to easterly over the central and southern SMO at low levels. A second northward movement into central Arizona and New Mexico results in easterlies being confined to Mexico, suggesting that moisture from the Gulf of Mexico makes little contribution to the monsoon rainfall over the southwestern United States, moisture having originated mainly from the Gulf of California and the eastern Pacific Ocean, which is similar to that in the study by Berbery (2001).

b. Discussion

In this study, the MM5–OSU model is shown to successfully reproduce the seasonal climatology of the North American monsoon system. While the simulation emphasized the heterogeneity of the precipitation, temperature, water content, and wind field within the NAMS region, it provided information relating to three questions. 1) What is the origin of low-level moisture that appears to be responsible for the seasonal development of NAMS? 2) How is the low-level circulation tied to the reversal of zonal wind direction from westerly to easterly? 3) How does the skin temperature develop with the precipitation variation in the NAMS region?

With respect to the first question, there has been much speculation, including discussion of the impact of enhanced moisture from the Gulf of Mexico associated

with the westward extension of the Bermuda high (Bryson and Lowry 1955; Sellers and Hill 1974), and the movement of low-level moisture into Arizona from the tropical eastern Pacific Ocean via the Gulf of California (Reitan 1957; Hales 1972; Douglas et al. 1993). Low-level moisture attributed largely to the Gulf of California, and the upper-level water vapor is transported from the Gulf of Mexico (Carleton 1986; Stensrud et al. 1995; Schmitz and Mullen 1996). The present study clearly suggests that the onset of rainfall in the central and southern SMO is closely related to the reversal of wind from westerly to easterly at a low level, with moisture contents originating mainly from the Gulf of Mexico. The onset of rainfall in the Sonoran Desert and the central areas of Arizona and New Mexico is associated with the reduction of westerlies, but the moisture content is still from the Gulf of California and the eastern Pacific Ocean in the weakening southwesterlies.

With respect to the second question, the present analyses show that the reversal of wind from westerly to easterly is largely associated with the rapid northward movement of the subtropical high over the North American Plateau. This subtropical high results from the westward and northward expansion of the Bermuda high and causes dry southwesterlies from the Pacific Ocean to be replaced by moist southeasterly winds. Notice that, although the subtropical high can reach central Arizona and New Mexico (leading to the reduction of westerlies), easterlies are still confined to Mexico. Hence, the rapid northward movement of the subtropical high over the Sierra Madre Occidental in Mexico is mainly responsible for the reversal of wind from westerly to easterly.

With respect to the third question, it is interesting to note that the temperature (Fig. 6) in central Mexico and south of the SMO decreases with the increase of monsoon rainfall, while the temperature in the southwestern United States did not decrease with an increase in monsoon rainfall. Locations north of the SMO have a similar precipitation onset date as locations in the northern NAMS (A and B), but a time evolution in temperature is similar to the southern NAMS (C and D). Apparently, the long-term mean temperature is independent from precipitation variation. This might be due to the fact that the temperature is tied to underlying surface characteristics while the precipitation field evolves along with the upper-atmosphere structure. This seems to be qualitatively supported by Figs. 7 and 9; that is, the time evolution of wind fields in the southwestern United States (A and B) and north of the SMO (C) seems to follow the onset of rainfall in the central (D) and southern SMO (E) and is associated with the movement of the subtropical high. On the other hand, due to the heterogeneity in the monsoon region, more frequent and stronger rainfall events (associated with the diurnal cycle or intraseasonal variability) occur in the southern NAMS (cf. Figs. 6b and 6a). The rainfall amount is much higher in the southern NAMS than that in the

northern NAMS (Fig. 3), which may subsequently lower the Bowen ratio, leading to decreased surface temperatures. In contrast, rainfall in the northern NAMS is less frequent and weaker in the 22-yr climatological mean, and the relatively higher Bowen ratio and temperature appear after the onset of precipitation.

Acknowledgments. The authors would like to thank NCAR's Scientific Computing Division (SCD) for supporting part of the calculation and providing the reanalysis data and the global SST data. A special thanks also goes to the Climate Prediction Center (CPC) for providing the real-time precipitation analysis data. Appreciation is extended to Mr. T. Matsui for providing the TOVS skin temperature data. The comments and suggestions offered by the two anonymous reviewers contributed to considerable improvement of the paper. This research is sponsored by NASA Grants NAG5-11044 and NAG5-9328, NOAA Grants NA16GP1605 and NA06GP0477, and SAHRA (NSF STC on "Sustainability of Semi-Arid Hydrology and Riparian Areas") Grant ERA-9876800.

REFERENCES

- Adams, D. K., and A. C. Comrie, 1997: The North American monsoon. *Bull. Amer. Meteor. Soc.*, **78**, 2197–2213.
- Anderson, B. T., 2002: Regional simulation of intraseasonal variations in the summertime hydrologic cycle over the southwestern United States. *J. Climate*, **15**, 2282–2300.
- , J. O. Roads, and S.-C. Chen, 2000a: Large-scale forcing of summertime monsoon surges over the Gulf of California and southwestern United States. *J. Geophys. Res.*, **105** (D19), 24 455–24 467.
- , —, —, and H.-M. H. Juang, 2000b: Regional simulation of the low-level monsoon winds over the Gulf of California and southwestern United States. *J. Geophys. Res.*, **105** (D14), 17 955–17 969.
- , —, and —, 2001: Model dynamics of summertime low-level jets over northwestern Mexico. *J. Geophys. Res.*, **106** (D4), 3401–3413.
- Barlow, M., S. Nigam, and E. H. Berbery, 1998: Evolution of the North American monsoon system. *J. Climate*, **11**, 2238–2257.
- Berbery, E. H., 2001: Mesoscale moisture analysis of the North American monsoon. *J. Climate*, **14**, 121–137.
- Bryson, R. A., and W. P. Lowry, 1955: The synoptic climatology of the Arizona summer precipitation singularity. *Bull. Amer. Meteor. Soc.*, **36**, 329–339.
- Carleton, A. M., 1986: Synoptic-dynamic character of "bursts" and "breaks" in the southwest U.S. summer precipitation singularity. *J. Climatol.*, **6**, 605–623.
- Chen, F., and J. Dudhia, 2001: Coupling an advanced land surface-hydrology model with the Penn State-NCAR MM5 modeling system. Part I: Model description and implementation. *Mon. Wea. Rev.*, **129**, 569–585.
- , Z. Janjic, and K. Mitchell, 1997: Impact of atmospheric surface-layer parameterizations in the new land-surface scheme of the NCEP mesoscale Eta Model. *Bound.-Layer Meteor.*, **85**, 391–421.
- Douglas, M. W., R. A. Maddox, K. W. Howard, and S. Reyes, 1993: The Mexican monsoon. *J. Climate*, **6**, 1665–1677.
- Dunn, L. B., and J. D. Horel, 1994a: Prediction of central Arizona convection. Part I: Evaluation of the NGM and Eta Model precipitation forecasts. *Wea. Forecasting*, **9**, 495–507.
- , and —, 1994b: Prediction of central Arizona convection. Part II: Further examination of the Eta Model forecasts. *Wea. Forecasting*, **9**, 508–521.
- Giorgi, F., 1991: Sensitivity of simulated summertime precipitation over the western United States to different physics parameterizations. *Mon. Wea. Rev.*, **119**, 2870–2888.
- , C. S. Brodeur, and G. T. Bates, 1994: Regional climate change scenarios over the United States produced with a nested regional climate model. *J. Climate*, **7**, 375–399.
- Gochis, D. J., W. J. Shuttleworth, and Z.-L. Yang, 2002: Sensitivity of the North American monsoon regional climate to convective parameterization. *Mon. Wea. Rev.*, **130**, 1282–1298.
- , —, and —, 2003: Hydrometeorological response of the modeled North American monsoon to convective parameterization. *J. Hydrometeorol.*, **4**, 235–250.
- Grell, G. A., 1993: Prognostic evaluation of assumptions used by cumulus parameterizations. *Mon. Wea. Rev.*, **121**, 764–787.
- , J. Dudhia, and D. R. Stauffer, 1994: A description of the fifth-generation Penn State/NCAR Mesoscale Model (MM5). NCAR Tech. Note NCAR/TN-398+STR, 117 pp.
- Gutzler, D., and Coauthors, 2004: *The North American Monsoon Model Assessment Project (NAMAP)*. NCEP Climate Prediction Center Atlas 11, 32 pp.
- Hales, J. E., Jr., 1972: Surges of maritime tropical air northward over the Gulf of California. *Mon. Wea. Rev.*, **100**, 298–306.
- Higgins, R. W., J. E. Janowiak, and Y. Yao, 1996: *A Gridded Hourly Precipitation Data Base for the United States (1963–1993)*. NCEP Climate Prediction Center Atlas 1, 47 pp.
- , Y. Yao, and X. Wang, 1997: Influence of the North American monsoon system on the United States summer precipitation regime. *J. Climate*, **10**, 2600–2622.
- Kain, J. S., and J. M. Fritsch, 1990: Convective parameterization for mesoscale model: The Kain-Fritsch scheme. *The Representation of Cumulus Convection in Numerical Models*, No. 46, Amer. Meteor. Soc., 165–170.
- Kalnay, E., and Coauthors, 1996: The NCEP/NCAR 40-Year Reanalysis Project. *Bull. Amer. Meteor. Soc.*, **77**, 437–471.
- Kanamitsu, M., and K. C. Mo, 2003: Dynamical effect of land surface processes on summer precipitation over the southwestern United States. *J. Climate*, **16**, 496–509.
- Lakshmi, V., and J. Susskind, 2000: Validation of TOVS land surface parameters using ground observations. *J. Geophys. Res.*, **105** (D2), 2179–2190.
- , —, and B. J. Choudhury, 1998: Determination of land skin temperatures, surface air temperature and humidity from TOVS HIRS2/MSU data. *Adv. Space Res.*, **22**, 629–636.
- Reitan, C. H., 1957: The role of precipitable water vapor in Arizona's summer rains. Tech. Rep. on the Meteorology and Climatology of Arid Regions 2, Institute of Atmospheric Physics, The University of Arizona, Tucson, AZ, 19 pp.
- Schmitz, J. T., and S. L. Mullen, 1996: Water vapor transport associated with the summertime North American monsoon as depicted by ECMWF analyses. *J. Climate*, **9**, 1621–1634.
- Sellers, W. D., and R. H. Hill, 1974: *Arizona Climate, 1931–1972*. The University of Arizona Press, 616 pp.
- Stensrud, D. J., R. L. Gall, S. L. Mullen, and K. W. Howard, 1995: Model climatology of the Mexican monsoon. *J. Climate*, **8**, 1775–1794.
- Susskind, J., and V. Lakshmi, 1997: Assessment of climate forcing using TOVS Pathfinder Path A data. Preprints, *Eighth Symp. on Global Change Studies*, Long Beach, CA, Amer. Meteor. Soc., 108–111.
- Tang, M., and E. R. Reiter, 1984: Plateau monsoons of the Northern Hemisphere: A comparison between North America and Tibet. *Mon. Wea. Rev.*, **112**, 617–637.
- Xu, J., and E. Small, 2002: Simulating summertime rainfall variability in the North American monsoon region: The influence of convection and radiation parameterizations. *J. Geophys. Res.*, **107**, 4727, doi:10.1029/2001JD002047.